Published in final edited form as:

Vet Pathol. 2020 May ; 57(3): 445–456. doi:10.1177/0300985820913265.

Spectrum of Post-Transplant Lymphoproliferations in NSG Mice and Their Association With EBV Infection After Engraftment of Pediatric Solid Tumors

Heather Tillman[1], **Peter Vogel**[1], **Tiffani Rogers**[2], **Walter Akers**[3], **Jerold E. Rehg**[1,*]

[1]Department of Pathology, St. Jude Children's Research Hospital, Memphis, TN

[2]Animal Resources Center, St. Jude Children's Research Hospital, Memphis, TN

[3]Center for *In Vivo* Imaging and Therapeutics, St Jude Children's Research Hospital, Memphis, TN

Abstract

Pediatric patients receiving solid organ transplants may develop lymphoproliferative diseases, including graft-versus-host disease (GvHD) and post-transplant lymphoproliferative diseases (PTLDs). We characterized lesions in 11 clinically ill NOD.Cg-*Prkdc*^{scid} *Il2rg*^{tm1Wjl}/SzJ (NSG) mice that received pediatric patient-derived solid tumors (PDXs) and developed immunodeficiency-associated lymphoproliferations comparable to GvHD and PTLDs over a period of 46 to 283 days post implantation. Lymphoproliferations were diffusely positive for human-specific biomarkers, including NUMA1, CD45, and CD43, but lacked immunoreactivity for murine CD45. Human immune cells were CD3-positive, with subsets having immunoreactivity for CD4 and CD8 as well as PAX5, CD79a, and IRF4, resulting from populations of human T and B cells present within the xenotransplants. Tissues and organs infiltrated included mucocutaneous zones (oral cavity, perigenital and perianal regions), haired skin, tongue, esophagus, forestomach, thyroid, salivary glands, lungs, liver, kidneys, spleen, lymph nodes, bone marrow, and brain. In 4/5 mice with PTLD, Epstein-Barr virus (EBV)-encoded small RNAs (EBERs) were detected by *in situ* hybridization in PAX5^{+} human B cells associated with the PDX (n = 1/4) or with engrafted human immune cells at other anatomic locations (n = 4/11). One of the 4 mice had an EBV-associated human large B-cell lymphoma. NSG mice receiving xenotransplants can develop combinations of GvHD, EBV-driven PTLD, and B-cell lymphoma similar to those occurring in human pediatric patients. Therefore, pediatric xenotransplants should undergo histopathologic and immunohistochemical assessment upon collection to ensure that the specimen is not a lymphoma and does not contain lymphoma cells, as these neoplasms can morphologically mimic small round blue cell pediatric solid tumors.

*Corresponding Author: Jerold Rehg, St Jude Children's Research Hospital, 262 Danny Thomas Place, Memphis, TN 38105, USA. Telephone: 901-595-2293. Fax: 901-595-3100. jerold.rehg@stjude.org.

AUTHOR CONTRIBUTIONS

H.T. and J.E.R. contributed to the conception or design of the report. All authors (H.T., P.V., T.F., W.A., J.E.R.) contributed to portions of the data acquisition and interpretation. H.T. and J.E.R. contributed to the drafting and critical revision of the manuscript.

CONFLICT OF INTEREST

No author declared a conflict of interest.

Keywords

Mice; NSG; graft-versus-host disease; post-transplant lymphoproliferative diseases; lymphoma; EBV

For several decades, since the discovery of the nude mouse, immunodeficient mouse strains have been used for human tumor implantation studies.[34] Implanting pieces of human tumors directly into severely immunocompromised NSG mice has become a popular modeling strategy for studying rare pediatric tumors and a tool for personalizing therapeutic approaches, as these xenografts more accurately recapitulate the biological features and drug responses of human neoplasms.[2,15,37] Consequently, patient-derived xenograft (PDX) mouse models are being used not only to investigate the mechanisms of tumor biology but also to improve the success of preclinical trials. The popularity of the NSG (NOD.Cg-*Prkdc*^{scid} *Il2rg*^{tm1Wjl}/SzJ) mouse is attributed to the fact that it is functionally T-, B-, and NK-cell deficient and has reduced innate immunity, including defects in dendritic and macrophage functions and multiple cytokine abnormalities related to the loss of IL-2-dependent signals.[41] However, there are limitations to using severely immunocompromised mice, such as NSG mice, as human disease models. The highly immunodeficient state of NSG mice renders them vulnerable to bacterial and viral infections, spontaneous mouse T-cell lymphomas, and the development of post-transplant lymphoproliferations, which may or may not be associated with infectious etiologies such as Epstein-Barr virus (EBV) (i.e., human gammaherpesvirus 4, the causative agent of infectious mononucleosis).[5,13,14,45,46] Experimentally induced lymphoproliferations and lymphomas can affect the data generated from preclinical studies and the ability to engraft and propagate rare tumors. Thus, it is necessary to recognize the pathogenesis of these lesions and develop strategies to deal with them when they are encountered.

Lymphoproliferative disorders comprise both benign and neoplastic proliferations of immunologically competent lymphoid and/or plasmacytic immune cells that develop in immunosuppressed hosts transplanted with solid tissue or allogenic hematopoietic cells. The World Health Organization (WHO) has devised a classification system for morphologic patterns consistent with transplant–associated lymphoproliferation that includes 1) nondestructive lesions caused by more benign lymphoid proliferations (plasmacytic hyperplasia, infectious mononucleosis–like hyperplasia, follicular hyperplasia) and 2) destructive lesions caused by malignant lymphoid proliferations (polymorphic or monomorphic [B-, T-, NK-cell types]. The destructive monomorphic B-cell lymphomas have morphologic features consistent with diffuse large B-cell lymphoma or classical Hodgkin lymphoma.[43] Although post-transplant lymphoproliferative diseases (PTLDs) encompass a spectrum of hyperplastic and malignant lesions, the PTLD designation is most frequently used to describe B-cell neoplasia; however, anaplastic T-cell neoplasms have also been described as PTLDs.[25] Most PTLDs are associated with viral infections, primarily EBV infection.[8,43] Indeed, the histologic lesions associated with most PTLDs, including the development of malignant subtypes such as diffuse large B-cell lymphoma, are mainly associated with EBV pathogenesis.

In pediatric patients, a primary EBV infection is considered the most common PTLD risk factor, and early treatment interventions are considered helpful in managing the disease.[8,27] EBV-infected naive B cells form germinal centers, leading to the persistent infection of memory B cells. These become immortalized and express latent viral proteins, including LMP1 and LMP2A-B,that are localized to the cell membrane. LMP1, a mimic of CD40, is considered the major oncogenic protein. Additionally, B cells latently infected with EBV express EBV-encoded small nonpolyadenylated RNAs (EBERs), which can be readily detected by *in situ* hybridization (ISH).[10,29]

Antibodies directed against EBV have been demonstrated in all human population groups. However, it appears that only 50% of children younger than 6 years are seropositive,[6,9] although this percentage increases with age. Approximately 66% of adolescents aged 13–14 years and 82% of individuals aged 18–19 years exhibit seropositivity, with the incidence in the latter group being similar to the 85% to 95% seropositivity observed in adult populations.[6,9] Studies aimed at understanding the risk factors for PTLD development in human patients are largely centered on the immune system responses that develop, especially when an EBV-negative recipient receives hematopoietic cells or solid tissue from a donor patient who is serologically positive for EBV.[27] Interestingly, recipient EBV status before transplant is not always correlative for developing PTLD in adult patients. However, in pediatric patients seronegativity is considered the most common indicator for the disorder, especially during the first year after transplantation.[8]

Among the many risk factors associated with PTLD development are immunosuppression associated with graft-versus-host disease (GvHD) therapy and prophylaxis, which may or may not be directly associated with infectious etiologies. The EBV-negative PTLDs that occur may be biologically distinct from the disease associated with EBV.[28,29] GvHD results from engrafted donor T lymphocytes responding to foreign host proteins on epithelia of multiple organs, but especially the skin, lung, liver, and gastrointestinal tract.[11] GvHD is most commonly reported in patients who have received allogeneic stem cell transplants. However, it may also occur in a subset of patients who fail to mount an effective response to immunologically competent lymphoid cells that may or may not be virus-infected and that are transplanted as part of a solid tissue, such as liver. GvHD may also occur concurrently with PTLD. Historically, when GvHD occurs within 100 days of transplantation it has been defined as acute GvHD (aGvHD). In both pediatric and adult patients, post-transplant–associated chronic GvHD (cGvHD), has generally been defined as occurring 100 days post-transplant. This temporal difference is no longer a defining criteria, and is considered an arbitrary distinction between the two disorders since it is now recognized that there is temporal overlap between these disorders.[11,12] cGvHD can coincide with the development of either early-onset (<2 years) or late-onset (>2 years) PTLD post-transplant.[19,35] When PTLD and GvHD occur simultaneously they may involve the same organs. Consequently, depending upon the organs involved it can be diagnostically challenging to distinguish these two conditions based on histologic lesions when they occur in the same host.[8] However, our data show that histopathologic examination of select tissues can aid in differentiating these two conditions when in the same host.

Here we report on a series of 11 NSG mice that developed atypical lymphoproliferations of human cells after receiving transplants of pediatric solid tumors. These lymphoproliferations were consistent with both GvHD-like lesions and EBV-positive and EBV-negative PTLD. NSG mice in which PTLD was diagnosed had both polymorphic and monomorphic lymphomatous proliferations. Our data provide the first demonstration of EBV- and non–EBV-associated post-transplant lymphoproliferations concurrent with EBV-negative GvHD arising from the transplantation of pediatric solid tumors into NSG mice. Our data further suggest that testing of pediatric xenografts for human lymphocyte markers and/or EBV contamination before implantation may be helpful in assessing the potential for a successful PDX engraftment. Our data show that PDX tumors removed at the end of a study should be examined more closely for these lymphoid and plasmacytic proliferations of human origin.

MATERIALS AND METHODS

Mice

The 11 NOD.Cg-*Prkdc*^{scid} *Il2rg*^{tm1Wjl}/SzJ (NSG) mice (JAX stock #005557) were obtained directly from The Jackson Laboratory (Bar Harbor, Maine) as part of a group of 32 mice that were used for transplantation studies.[7,42]. The mice in this report were females aged 14 to 52 weeks. All mice were housed at St. Jude Children's Research Hospital (St. Jude) under strict specific pathogen–free barrier practices with sterilized water, food (Autoclavable Rodent Lab Diet 5013, Lab Diet, St. Louis, MO.), bedding (Anderson Bedo-cob, Maumee, OH.), and positively-pressure-ventilated microisolation cages (Allentown Caging, Allentown, NJ.), automatic 12hr light-dark cycle of 0600 to 1800 hr, a minimum of 15 air changes/hr, administration of amoxicillin [0.25 mg/mL] in the water), and handling using aseptic techniques including the use of laminar flow hoods, personal protective equipment, and hair coverings, because of their increased susceptibility to opportunistic bacterial infections.[13] Mice were tested and reported to be negative for the following pathogens: *Helicobacter* spp., *Mycoplasma pulmonis, Pneumocystis carinii*, Sendai virus, mouse parvovirus (MPV), mouse hepatitis virus (MHV), minute virus of mice (MVM), Theiler murine encephalomyelitis virus, epizootic diarrhea of infant mice (EDIM), pneumonia virus of mice (PVM), reovirus, K virus, polyoma virus, lymphocytic choriomeningitis virus (LCMV), mouse adenovirus (MAV), ectromelia virus, and murine ecto- and endoparasites. Mice were assigned to animal protocols approved by the St. Jude Institutional Animal Care and Use Committee. The mice used in this report were associated with research conducted by the Pediatric Solid Tumor Network patient-derived tumor bank and by the Center for *In Vivo* Imaging and Therapeutics at St. Jude, which involves xenograft transplantation studies of various pediatric solid tumors. The implanted PDX specimens were taken from fresh surgically excised primary tumors.[30] The EBV status of the PDXs was not determined prior to engraftment and the tumor specimens were surgically implanted into the subcutaneous flank tissue of the NSG mice. The mice included in this report initially demonstrated clinical illness defined as being hunched with alopecia. The animals were submitted for pathologic evaluation because of a clinical suspicion of an opportunistic infection. Mice were euthanized in an atmosphere of 100% CO_2.

Clinical Pathology and Microbiology Data

Using an intracardiac collection technique as a terminal procedure while under anesthesia, whole blood was collected into tubes with EDTA anticoagulant (BD Microtainer, BD Diagnostics) for a complete automated blood count analysis (CBC) and a peripheral blood smear. Approximately 20 μL of EDTA-treated blood was used for analysis on the ForCyte Hematology Analyzer (Oxford Science, Inc.). Peripheral blood smears were prepared and methanol fixed, and a Wright–Giemsa stain was applied. For the aerobic blood culture, 50–75 μL of blood was obtained separately and placed in an aerobic bottle using aseptic technique. Additional select tissues (lungs, synovial fluid) samples were aseptically collected for aerobic cultures and subsequently analyzed. The available CBC analyses, peripheral blood smears, and microbiology data for all mice were reviewed and interpreted by a board-certified veterinary pathologist (H.T.).

Histopathology

Tissues from all major organs (heart, lungs, tongue, kidneys, liver, spleen, lymph nodes, residual thymic tissue, esophagus, oropharyngeal tissue, stomach, salivary glands, Harderian glands, adrenal glands, thyroid gland, pancreas, pituitary gland, small intestine, large intestine, ovaries, uterus, urinary bladder, eyes, brain, spinal cord, sternum, femur, tibia) were collected and processed for histopathologic evaluation. All tissues were fixed in 10% neutral-buffered formalin, embedded in paraffin, sectioned at 4 μm, and stained with hematoxylin and eosin. Bony tissues were decalcified in 10% formic acid. Stained sections were reviewed by light microscopy and interpreted by three board-certified veterinary pathologists (H.T., J.E.R., and P.V.). Human cellular infiltrates within a tissue were scored by visual estimation of NUMA1H-positive cells as follows: within normal limits (<1%), minimal (1-10%), mild (11-25%), moderate (26-50%), marked (51-75%) or severe (>75%).

Immunohistochemistry and In Situ *Hybridization*

All formalin-fixed, paraffin-embedded (FFPE) tissues were sectioned at 4 μm, mounted on positively-charged glass slides (Superfrost Plus; Thermo Fisher Scientific, Waltham, MA), and dried at 60°C for 20 min. Procedures and antibodies used to detect human or mouse hematolymphoid antigens to NUMA1H (human specific), CD45H (human specific), CD43H (human specific), CD4H (human specific), CD8H (human specific), CD79aH (human specific), CD68H (human specific), CD3ε, PAX5, IRF4, F4/80, and CD45M (mouse specific) are listed in Table 1. Human tonsil and mouse spleen were used as positive IHC controls. EBERs are the only gene products expressed throughout all latent and lytic phases of the viral infection cycle, and they are the most reliable markers of EBV infection.[29] EBER mRNAs were detected by *in situ* hybridization (ISH) with a probe for EBV-encoded small RNAs (EBER Probe, Leica Biosystems, catalog # PB0589), using the Leica BOND RX automated stainer. A control poly-A probe was used to check for RNA integrity, and a proven EBV-driven lymphoma was used as a positive control for EBER signal. Probes for the human kappa light chain mRNA (Kappa Probe, Leica Biosystems, catalog # PB0645) and human lambda light chain mRNA (Lambda Probe, Leica Biosystems, catalog # PB0669) were used to assess B-cell clonality, using the Ventana Benchmark XT automated stainer.

Human tonsil was used as a positive immunoglobulin light-chain control. The conditions for the ISH using chromogenic detection methods are listed in Table 2.

RESULTS

Clinical Status of PDX NSG Mice With Lymphoproliferative Disorders

The clinical characteristics, transplant information, and EBV status of NSG mice in which a lymphoproliferative disorder was diagnosed are presented in Table 3. Seven of the 11 mice had concurrent bacterial growth, but histopathologic pathologic changes consistent with a bacterial infection were not apparent. Additionally, 10 of the 11 mice had elevated leukocyte counts when compared with in-house (0.9×10^3/μL to 2.96×10^3/μL) and published reference intervals for this mouse strain.[42]

Distribution and Characterization of Human Lymphoid and Plasmacytic Multisystemic Proliferations

Table 4 shows the anatomic distributions of the lymphoproliferations in the 11 mice. The lymphoid cells in these mice expressed NUMA1H, CD45H, CD43H, and varying combinations and concentrations of CD3, CD4H, and CD8H. Also, these cells lacked expression of CD45M, indicating that they were of human origin and had originated from the xenografts transplanted from pediatric donors. The human lymphocytes in the cutaneous and mucocutaneous locations predominately expressed CD3 and CD4H with strong intensity; far fewer cells expressed CD8H or CD79aH. The lungs of all 11 mice had scant to marked perivascular and peribronchiolar lymphoid infiltrates, with patchy involvement of the interstitial septa in 3 mice. In the lungs of 8 mice, the pulmonary infiltrates consisted of lymphocytes and plasma cells, with the plasma cells being abundant. Other tissues (the thyroid gland, salivary glands, Harderian gland, Zymbal's gland, pancreas, liver, skeletal muscle, and nervous system including brain, nerves, and ganglia) had varying concentrations of human lymphocytic infiltrates with immunophenotypes comparable to those found in cutaneous and mucocutaneous tissues and morphologic patterns consistent with GvHD. Two of the 11 mice had segmental human lymphoid infiltrates within the duodenal lamina propria without tissue destruction. There was no evidence of infiltrates or lesions within the large intestines of any of the 11 mice.

Unlike the squamous and mucocutaneous tissues, the infiltrates in the lungs of 6 of the 11 mice consisted of a mixture of T cells and an abundance of plasma cells. The pulmonary T-cell population was diffusely $CD3^+$, with a CD4H to CD8H ratio of 2 or 3 to 1 as determined by visual estimation. The plasma cells were strongly positive for CD79aH and/or IRF4. The lung infiltrates of the other 5 mice were predominantly $CD4H^+$ T-cell lymphocytes. Cellular infiltrates of human T-cell lymphocytes were observed in 1 or more neural tissues in 6 of the 11 NSG mice. $CD3^+$ and $CD4H^+$ T cells were identified in meninges, midbrain parenchyma, and cranial and peripheral nerves and ganglia. Unexpectedly, we observed mild to moderate perimysial lymphocytic infiltrates in various skeletal muscles. These lymphocytes expressed NUMA1H, CD3, and CD4H and/or CD8H, consistent with their being of human origin.

In tissues with stratified squamous epithelium, such as mucocutaneous and mucosal locations, as well as haired skin, the lymphocytic infiltrates formed a lichenoid, interface pattern that was characterized by lymphocytes invading the basal layer of the epithelium in mucosal and cutaneous locations as well as the pilosebaceous units within the skin (Figure 1). Dyskeratotic and apoptotic cells were visible in the skin, and 2 mice had subepithelial cleft formation (Figure 2). There were also bands of infiltrates visible in the mid-dermis. The findings for the haired skin were consistent with the clinical history and gross findings of progressively worsening alopecia (not shown). These lymphoid infiltrates were mixtures of $CD4H^+$ cells (Figure 3 with fewer $CD8H^+$ cells (Figure 4). $CD79aH^+$ cells were rare, and the macrophages present in the lesions were of mouse origin, expressing F4/80 and being negative for human-specific CD68.

The parotid and/or submandibular salivary glands and other glandular tissues had variable involvement, with inflammatory cell infiltrates consisting predominantly of human lymphocytes admixed with minimal numbers of $IRF4^+$ plasma cells, $CD79aH^+$ cells, and occasional neutrophils. In addition to the lymphocytes invading the ductal epithelium, there was also necrosis of the ducts and acini. The thyroid glands in 8 of the 11 mice had extensive infiltrates consisting predominately of human lymphocytes (and less often plasma cells) that effaced the glands (Figures 5 and 6). Again, the lymphoid infiltrates at these locations also expressed NUMA1H, CD3, CD45H, CD4H, or CD8H. In all cases, CD4H cells were the dominant lymphocyte. The plasma cells expressed CD79aH and/or IRF4.

The splenic white pulp of healthy NSG mice is markedly hypoplastic. In contrast, there was lymphocyte expansion of the white pulp in 6 of the 11 mice. In 2 of these mice, there was lymphoplasmacytic expansion of the white pulp with extension into the red pulp. The lymph nodes of healthy NSG mice are rudimentary, small, and devoid of lymphoid cells. The lymph nodes in 7 of 9 xenotransplanted NSG mice underwent progressive changes consisting of an increase in lymphoid cells (hyperplasia), mixing of intact and necrotic lymphoid cells (necrotizing lymphadenitis), and atrophic sclerosing lymphadenitis. The lymphoid population in the cellular and mixed lymph nodes comprised $CD45H^+$ cells that expressed either CD4H or CD8H and plasma cells that expressed CD79aH and IRF4. In 3 of the 11 mice, the bone marrows were hypoplastic with very few to no mouse (host) cells but a mild to moderate number of $CD4H^+$ cells throughout the medullary cavity (Figure 7).

NSG Mice Are Susceptible to Developing GvHD and EBV-Positive or EBV-Negative PTLDs

All of the 11 mice had lymphoid infiltrates with morphologic patterns that were characteristic of GvHD or GvHD with destructive and nondestructive PTLD based on the WHO classification for PTLDs, and 5 mice had features characteristic of human PTLD subtypes.[43] Morphologic changes occurred within the keratinized squamous covering organs (the skin, tongue, esophagus and forestomach) in all 11 mice. Eight of the 11 mice had lesions involving mucocutaneous tissues (the oral cavity, anus, and vulva), and all 11 had lung lesions. In 4 of the 11 PDX mice, the implantation site exhibited histologic changes characterized by a lymphoma or dense lymphoplasmacytic infiltrates of human cells that effaced or replaced the xenograft in remission. Neither intact nor resolving PDX tissue was evident at the implantation sites in the other 7 PDX mice. As observed in other tissues with

GvHD but not lymphoma, the lymphoplasmacytic infiltrates at the implantation site were composed primarily of cells that expressed CD4H and/or CD8H, with the former predominating, which is consistent with cGvHD. Only a few cells expressed CD79aH or IRF4. Comparable combinations of lymphoid and plasmacytic proliferations with or without lymphoma were observed in some tissues distant from the transplant site.

Because EBV infection has been associated with the development of lymphoproliferations in humans, we assessed the EBV status of lymphoid infiltrates in NSG mice that received xenotransplants by using HE staining, IHC, and EBV ISH (Figures 8-11). Tissues with lymphoid infiltrates suggestive of GvHD were examined for the presence of EBV which included lungs (n = 11), spleen (n = 9), lymph nodes (n = 7), haired skin (n = 9), tongue (6), esophagus (8), thyroid glands (8), salivary glands (8), brain (n =5), forestomach (n = 7), and bone marrow (n = 3). EBER signal was not detected in any of these tissues.

Four of the 11 mice with lesions consistent with GvHD had atypical lymphocytes unrelated to the GvHD that were positive for EBERs by ISH (Table 3).[21,32,36] Specifically, depending on the tissue, 75% to 90% of the B cells populating 4 of the 5 cases with either polymorphic or monomorphic PTLD had a strong EBER signal. In the lungs of the 3 mice with small, focal features of polymorphic PTLD, most PAX5-expressing cells also showed a strong signal for EBER.

Two of the 11 mice with minimal or extensive tissue lesions consistent with GvHD also had a monomorphic PTLD containing a large B-cell lymphoma. The lymphoma of both mice involved the spleen, liver, lymph nodes and 1 of the 2 lymphomas also involved the spinal cord and the PDX implantation site. One of 2 mice with monomorphic PTLD had a large B-cell lymphoma with anaplastic features that was positive for PAX5 and EBV (Figures 12-15). Clonality was assessed by evaluating kappa and lambda immunoglobulin light chain expression. This particular lymphoma was negative by ISH for both kappa and lambda light chain production, which is indicative of a clonal lymphoma. The second, monomorphic large B-cell lymphoma (Figure 16), arising in a different mouse, was PAX5 positive but negative for EBV. However, clonality was also assessed by ISH for kappa (Figure 17) and lambda (Figure 18). The EBV-negative lymphoma was lambda restricted by ISH, with a kappa:lambda ratio of 1:12 by visual assessment. Additionally, 3 of the 11 mice with GvHD also had lesions that were consistent with an EBV-positive polymorphic PTLD. One of the 3 mice had ISH light chain restriction with a kappa:lambda ratio of 8:1. The kappa:lambda ratio of the other 2 mice approximated the standard human 2:1 ratio as determined by visual assessment.

The 4 mice with EBV-positive PTLDs had multiple lung and splenic foci composed of mixed populations of mature and immunoblastic lymphocytes and plasma cells that varied in their proportion of CD3, CD4H, CD8H, PAX5, CD79aH, and EBERs signals. Some of the cells had atypical, large vesicular nuclei with prominent nucleoli. One of these 4 EBV-positive mice had combinations of lymphocytes and extranodal plasma cells throughout its lungs and spleen. There were numerous, localized, small lymphocytes with occasional atypical immunoblastic features. Additionally, 2 of the 4 EBV-positive mice had multiple pulmonary nodules with features of polymorphic PTLD, again characterized by

heterogeneous populations of both plasma cells, and small to intermediate-sized lymphocytes with occasional immunoblastic and atypical morphology. The fourth EBV-positive mouse had a monomorphic PTLD consisting of multiple nodules, characterized as a large B-cell lymphoma with anaplastic cells. This lymphoma also involved the spleen, liver, lymph nodes, and implantation site, with extension and invasion into the vertebrae and spinal cord. A fifth mouse had an EBV-negative monomorphic PTLD with histopathology that was comparable to the EBV-positive large B-cell lymphoma. There was also involvement of the spleen, the liver, and an abdominal lymph node. The polymorphic and monomorphic PTLDs expressed PAX5, CD79aH, and IRF4, which is consistent with a B-cell origin. A few $CD3^+$ T cells were scattered throughout the lymphoma.

DISCUSSION

The NSG strain is considered an essential tool for studying both normal and abnormal immunologic conditions, understanding oncogenesis, and investigating the effects of combinatorial therapies, because the model readily engrafts various human cells. However, the use of the NSG mouse for these types of study is not without its challenges and limitations. Our data show that human-derived lymphoproliferations can arise in NSG mice transplanted with pediatric solid tumors, because these mice are so permissive to engraftment as a result of their severe immunodeficiency. It is apparent from our data and those of others that implantation of PDX tumors can result in several outcomes. Ideally, a tumor implant will become well established and grow without causing clinical illness in the host mouse, replicating important biological aspects of the human disease. However, a PDX tumor may fail to grow, instead resolving in conjunction with the mouse developing xenogeneic GvHD, a PTLD, or a combination of these 2 diseases. We observed these outcomes in 11 of 32 (34%) mice that were transplanted as part of a year-long study.

In this report, the NSG mice implanted with various pediatric solid tumors developed lesions morphologically indicative of GvHD and destructive PTLD, due to the systemic engraftment of lymphocytes and plasma cells. These resulted in the development of a human large B-cell lymphoma in at least 2 cases.[40] Our observations in these NSG mice are similar to those reported for cases of PTLD in humans and after transplantation of adult solid tissues into NOD.Cg-*Prkdc*^{scid}*Il2rg*^{tm1Sug}/JicTac (NOG) and other immunocompromised mice.[5,36] Therefore, it appears that NSG mice, like humans, can develop a pathologic spectrum of PTLD phenotypes comparable to lesions described in the 2016 World Health Organization (WHO) system for classifying hematopoietic neoplasms.[43] However, we did not observe mice with hyperplasias or invasive T-cell lymphomas, which may occur in the human disease setting. Most human cases of PTLD are associated with EBV-driven B cells, although EBV-infected T cells and EBV-negative lymphoproliferations of B and T cells also occur and are also classified as PTLDs.[29,43] We also observed a correlation between the expression of EBERs and the development of these lymphoproliferations in a subset of NSG mice. Transplant donor cells are commonly the source of the PTLDs that occur in human patients receiving solid organ transplants, while the cells associated with PTLD in the mice in this report originated from the PDX. The lesions in our cohort were also consistent with other reports of adult-associated xenogeneic PTLD arising in transplanted NSG and NOG mice.[3,5,36]

All 11 of our NSG mice developed lesions in the skin, other squamous epithelial lined tissues, thyroid gland, salivary glands, lungs, CNS, bone marrow, lymph nodes, and liver, with apoptosis being evident in the skin and in other tissues with squamous epithelium. The pathology and organ distribution of the lymphoplasmacytic infiltrates in these 11 mice was consistent with GvHD.[1,24,36,39] The target-organ distribution of GvHD may differ among xenograft models depending on the mouse strain, the route of donor-cell administration, and differences in the source or type of the donor cells.[18,22,24,39] The pathology of both acute and chronic mouse models of GvHD relies on T-cell reactivity. However, the two forms of the disease have different phenotypes owing to the differential involvement of CD8+ or helper CD4+ T-cell subsets. In humans, GvHD is classified as aGvHD, which has been historically considered to occur within 100 days of transplant, or cGvHD, which develops 100 or more days after transplant but may take several years to become evident clinically.[40] However, this temporal difference is no longer a definitive feature in humans and it does not necessarily translate to GvHD in mice. cGvHD can develop within weeks after transplant in mice.[39] Consequently, it is not possible to differentiate aGvHD and cGvHD based on the time period over which disease occurs or the tissue distribution of the GvHD lesions. In human and mouse allograft GvHD, donor CD8+ T cells are activated when their T-cell receptor binds to recipient peptides presented in the context of recipient major histocompatibility complex I (MHC-I) molecules. However, most xenogeneic GvHD is dependent on donor antigen-presenting cells (APC). The predominance of CD8+ cells in all reported immunodeficient mouse models of human peripheral blood mononuclear cell (PBMC) engraftment suggests that strong reactivity against host (mouse) MHC-I is present.[1,24,47] Xenogeneic transplants of adult human solid organs in NSG mice also require human APCs to process mouse antigen and present them in the presence of MHC molecules. It has been hypothesized that human CD4+ T-cell expansion in immunodeficient mice is driven by human anti-mouse MHC-II reactivity.[44] Other investigators have indicated that T-cell recognition of MHC molecules is species restricted and that human T-cell receptors do not recognize mouse MHC molecules, thus making xenogeneic GvHD primarily a human CD4+ T-cell dependent response.[39,50] The infiltrates in the GvHD lesions in our 11 mice consisted primarily of human CD4+ T cells in association with a tissue-dependent variable number of human CD8+ T cells, which is consistent with cGvHD. cGvHD also involves B-cell stimulation, which would also account for the lymphoplasmacytic features prominent in some tissues of the mice in our report. It has been suggested the CD8+ T-cell presence may represent an early stage of the disease. It has also been speculated that the presence of both CD4+ and CD8+ T cells indicates that reactivity to mouse MHC I and MHC II may occur.[24] A recent study supporting this speculation demonstrated that xenogeneic GvHD did not develop in NSG mice deficient in MHC class I and II expression that were engrafted with human cells.[4] Furthermore, these data suggest that GvHD associated with the proliferation of human T cells engrafted into immunodeficient mice (NOD-*scid*, NOG, NSG) is a response to stimulation by host (mouse) MHC I and MHC II molecules.[24]

The high levels of human CD4+ T cells with low levels of CD8+ human T cells associated with the GvHD observed in the 11 mice in our report mimic the immunophenotype reported by others and suggest that the GvHD in our mice comprised overlapping aGvHD and cGvHD. This observation is consistent with the overlapping syndrome of GvHD in some

human patients.[11,12] The epitheliotropic human CD4 T-cell infiltrates in the skin, tongue, esophagus, forestomach, thyroid glands, and salivary glands are features consistent with cGvHD. Three mice in our report had bone marrow hypoplasia, 3 mice had severe sclerosing lymphadenitis, and 5 mice had meningoencephalitis. These lesions observed in the present report further suggest that CD8+ aGvHD was present at some point. Bone marrow hypoplasia has been reported to occur in GvHD in xenogeneic NSG mice, as well as in human patients.[1,16,18,24,48]

The GvHD in our NSG mice differed in several ways from that reported by others. GvHD of the gastrointestinal tract characterized by gastritis and/or enterocolitis is a common hallmark of GvHD in humans and mice.[18,24,39,40,47] A mild infiltrate of human CD4+ T cells in the lamina propria of the duodenum was observed in only 2 of our report mice, with no tissue damage or evidence of apoptosis. However, there was involvement of the tongue, esophagus, and forestomach, all of which are lined by squamous epithelium. Myositis has been reported in human GvHD[40] but, to the authors' knowledge, it has not been previously reported in mouse GvHD models; however, 45% (5 of 11) of our report mice had lymphocytic infiltrates in their skeletal muscles. Although the central nervous system (CNS) is a target of acute allogeneic GvHD in mice (but rarely in human patients), CNS involvement has not, to our knowledge, been previously reported in xenogeneic GvHD.[17,20,38] However, 7 of our 11 report mice had human T lymphocytes present in 1 or more CNS tissues (brain parenchyma, meninges, cranial nerves, and/or peripheral nerves and the cranial nerve, dorsal root and paraspinal ganglia). The authors are aware of only 1 report of thyroiditis associated with xenogeneic GvHD in mice, whereas thyroiditis was observed in 8 of 11 of our NSG report mice.[36] The same 8 mice also had a moderate to marked sialadenitis, which is common in human patients and is mentioned in only a few reports of xenogeneic GvHD in mice.[18,36] The difference in the range of tissues involved in our mice compared to those reported previously may be attributed to the limited tissue sets that were collected and evaluated in other mouse studies. The tissues assessed in some studies were limited to the skin, lungs, liver, and gastrointestinal tract.[24,26,39,47] Natural variation in disease expression may also account for some of the differences between tissue targets identified in our report and those identified in other studies.

Our data indicate that NSG mice engrafted with pediatric solid tumor xenografts may develop a spectrum of lymphoproliferations that are consistent with GvHD and one or more of the PTLDs as classified by the WHO.[43] The data further suggest that xenogeneic GvHD can be a limiting factor in the engraftment of pediatric solid tumors in NSG mice, as it has been reported to be for NSG mice receiving mononuclear cells from patients with acute myeloid leukemia or human PBMCs and for NOG mice receiving patient-derived melanoma cells.[1,36,49] Similarly, our data suggest that PTLDs can also be a limiting factor to PDX engraftment, especially when the PDX harbors EBV-infected lymphocytes. It is apparent that either condition can have an adverse effect on the successful engraftment of PDX tumors and can lead to the false interpretations that a lymphoma at the implantation site is a successful PDX tumor engraftment, or that the lack of PDX development is a positive effect of a therapeutic drug. It has been documented that 40% of PDX samples contain B and T lymphocytes and macrophages.[33,51] Therefore, to help minimize these potential problems, it has been recommended that PDX specimens be assessed for the presence of human0

lymphocytes before being implanted in NSG mice.[3] However, others have found this approach to be unhelpful in preventing these diseases.[23] This is not surprising, as just 1 EBV-positive B cell in a pool of 4×10^6 B cells can generate a lymphoma in SCID mice.[31] We have recently documented that T-cell lymphomas can arise spontaneously in NSG mice and that they can arise in conjunction with a human xenograft tumor.[45] Consequently, at the end of a study, we recommend that PDX tumors that are continuously transferred in mice should be assessed for the presence of mouse lymphoma cells or human lymphoproliferations. Histopathologic assessment of pediatric solid tumors without immunohistochemical assessment is not sufficient to ensure the PDX is not a lymphoma, because a lymphoma can morphologically mimic many so-called small round blue cell pediatric tumors, such as undifferentiated epithelial tumor, neuroblastoma, desmoplastic round cell tumor, Ewing sarcoma, and rhabdomyosarcoma.

In summary, NSG mice transplanted with xenogeneic pediatric PDX solid tumors may develop lymphoproliferative diseases associated with their severe combined immunodeficiency phenotype. Our data show that systemic lymphoid and lymphoplasmacytic infiltrates, with features of PTLD that are associated with EBV infection of B lymphocytes or are the result of xenogeneic GvHD, may arise in NSG mice. Our findings further suggest that lymphocytes that express PAX5 and have EBV expression are more characteristic of PTLD in NSG mice, like in human pediatric patients and that they have unique morphologic features that can distinguish PTLD from xenogeneic GvHD. However, as both conditions may occur in the same mouse, immunophenotyping of the lymphocyte infiltrates in the skin, tongue, esophagus, forestomach, thyroid, and salivary glands is necessary if it is important to distinguish the 2 disorders. A heterogeneous lymphocyte population of human CD4+ and CD8+ T cells coupled with a distinctive tissue distribution provides more substantial evidence for xenogeneic cGvHD occurring alone without PTLD development or in combination with a PTLD.

ACKNOWLEDGEMENTS

The authors would like to thank Dr. John Choi for his input and discussions on human lymphoproliferative disorders and Keith A. Laycock, PhD, ELS for his editorial assistance. Additionally, the authors would like to thank the following individuals: the members of the St. Jude Veterinary Pathology Core Laboratory and Meifen Lu for their excellent technical support.

FUNDING

This report was partially supported by the National Cancer Institute of the National Institutes of Health under award numbers P30CA021765 and R50CA211481 (to W.J.A.). The work was also supported in part by the American Lebanese Syrian Associated Charities (ALSAC). The content is solely the responsibility of the authors and does not necessarily represent the official views of the National Institutes of Health.

REFERENCES

1. Ali N, Flutter B, Sanchez Rodriguez R, et al. Xenogeneic graft-versus-host-disease in NOD-*scid* IL-2Rγ^{null} mice display a T-effector memory phenotype. PLoS One. 2012;7(8):e44219. [PubMed: 22937164]
2. B Bertotti A, Migliardi G, Galimi F, et al. A molecularly annotated platform of patient-derived xenografts ("xenopatients") identifies HER2 as an effective therapeutic target in cetuximab-resistant colorectal cancer. Cancer Discov. 2011;1(6):508–523. [PubMed: 22586653]

3. Bondarenko G, Ugolkov A, Rohan S, et al. Patient-derived tumor xenografts are susceptible to formation of human lymphocytic tumors. Neoplasia. 2015;17(9):735–741. [PubMed: 26476081]
4. Brehm MA, Kenney LL, Wiles MV, et al. Lack of acute xenogeneic graft-versus-host disease, but retention of T-cell function following engraftment of human peripheral blood mononuclear cells in NSG mice deficient in MHC class I and II expression. FASEB J. 2019;33(3):3137–3151. [PubMed: 30383447]
5. Chen K, Ahmed S, Adeyi O, Dick JE, Ghanekar A. Human solid tumor xenografts in immunodeficient mice are vulnerable to lymphomagenesis associated with Epstein-Barr virus. PLoS One. 2012;7(6):e39294–e39294. [PubMed: 22723990]
6. Condon LM, Cederberg LE, Rabinovitch MD, et al. Age-specific prevalence of Epstein-Barr Virus infection among Minnesota children: effects of race/ethnicity and family environment. Clin. Infect. Dis 2014;59(4):501–508. [PubMed: 24820696]
7. Coughlan AM, Harmon C, Whelan S, et al. Myeloid engraftment in humanized mice: impact of granulocyte-colony stimulating factor treatment and transgenic mouse strain. Stem Cells Dev. 2016;25(7):530–541. [PubMed: 26879149]
8. Dierickx D, Habermann TM. Post-Transplantation Lymphoproliferative Disorders in Adults. N Engl J Med 2018;378: 549–562. [PubMed: 29414277]
9. Dowd JB, Palermo T, Brite J, McDade TW, Aiello A. Seroprevalence of Epstein-Barr Virus Infection in U.S. Children Ages 6-19, 2003-2010. PLoS One 2013;8: e64921. [PubMed: 23717674]
10. Elgui de Oliveira D, Müller-Coan BG, Pagano JS. Viral carcinogenesis beyond malignant transformation: EBV in the progression of human cancers. Trends Microbiol. 2016;24(8):649–664. [PubMed: 27068530]
11. Ferrara JLM, Levine JE, Reddy P, Holler E. Graft-versus-host disease. The Lancet. 2009;373(9674):1550–1561.
12. Filipovich AH, Weisdorf D, Pavletic S, et al. National Institutes of Health Consensus Development Project on criteria for clinical trials in chronic graft-versus-host disease: I. Diagnosis and Staging Working Group Report. Biol. Blood Marrow Transplant 2005;11(12):945–956. [PubMed: 16338616]
13. Foreman O, Kavirayani AM, Griffey SM, Reader R, Shultz LD. Opportunistic bacterial infections in breeding colonies of the NSG mouse strain. Vet. Pathol 2011;48(2):495–499. [PubMed: 20817888]
14. Fujii E, Kato A, Chen YJ, Matsubara K, Ohnishi Y, Suzuki M. Characterization of EBV-related lymphoproliferative lesions arising in donor lymphocytes of transplanted human tumor tissues in the NOG mouse. Exp. Anim 2014;63(3):289–296. [PubMed: 25077758]
15. Gao H, Korn JM, Ferretti S, et al. High-throughput screening using patient-derived tumor xenografts to predict clinical trial drug response. Nat. Med 2015;21(11):1318–1325. [PubMed: 26479923]
16. Godder K, Pati AR, Abhyankar SH, Lamb LS, Armstrong W, Henslee-Downey PJ. *De novo* chronic graft-versus-host disease presenting as hemolytic anemia following partially mismatched related donor bone marrow transplant. Bone Marrow Transplant. 1997;19(8):813–817. [PubMed: 9134174]
17. Grauer O, Wolff D, Bertz H, et al. Neurological manifestations of chronic graft-versus-host disease after allogeneic haematopoietic stem cell transplantation: report from the Consensus Conference on Clinical Practice in chronic graft-versus-host disease. Brain. 2010;133(10):2852–2865. [PubMed: 20846944]
18. Greenblatt MB, Vbranac V, Tivey T, Tsang K, Tager AM, Aliprantis AO. Graft versus host disease in the bone marrow, liver and thymus humanized mouse model. PLoS One. 2012;7(9):e44664. [PubMed: 22957096]
19. Gwon JG, Kim YH, Han DJ: Different causes of early and late-onset post transplant lymphoproliferative disorder in kidney transplantation patients after 2000. Asian J Surg. 2019;42: 551–556. [PubMed: 30327178]
20. Hartrampf S, Dudakov JA, Johnson LK, et al. The central nervous system is a target of acute graft versus host disease in mice. Blood. 2013;121(10):1906–1910. [PubMed: 23299314]

21. Hjalgrim H F J, Melbye M. The epidemiology of EBV and its association with malignant disease In: Arvin A, Campadelli-Fiume G, Mocarski E, Moore PS, Roizman B, Whitley R, Yamanishi K, ed. Human Herpesviruses: Biology, Therapy, and Immunoprophylaxis. Cambridge: Cambridge University Press; 2007.
22. Ito R, Katano I, Kawai K, et al. Highly sensitive model for xenogenic GVHD using severe immunodeficient NOG mice. Transplantation. 2009;87(11):1654–1658. [PubMed: 19502956]
23. John T, Yanagawa N, Kohler D, et al. Characterization of lymphomas developing in immunodeficient mice implanted with primary human non–small cell lung cancer. J. Thorac. Oncol 2012;7(7):1101–1108. [PubMed: 22617243]
24. King MA, Covassin L, Brehm MA, et al. Human peripheral blood leucocyte non-obese diabetic-severe combined immunodeficiency interleukin-2 receptor gamma chain gene mouse model of xenogeneic graft-versus-host-like disease and the role of host major histocompatibility complex. Clin. Exp. Immunol 2009;157(1):104–118. [PubMed: 19659776]
25. La Fortune K, Zhang D, Raca G, Ranheim EA. A unique "composite" PTLD with diffuse large B-Cell and T/anaplastic large cell lymphoma components occurring 17 years after transplant. Case Rep. Hematol 2013;386147–386147. [PubMed: 23738160]
26. Laing ST, Griffey SM, Moreno ME, Stoddart CA. CD8-positive lymphocytes in graft-versus-host disease of humanized NOD.Cg-Prkdc^{scid} Il2rg$^{tm1Wjl/SzJ}$ mice. J. Comp. Pathol 2015;152(2):238–242. [PubMed: 25670669]
27. Landgren O, Gilbert ES, Rizzo JD, et al. Risk factors for lymphoproliferative disorders after allogeneic hematopoietic cell transplantation. Blood. 2009;113(20):4992–5001. [PubMed: 19264919]
28. Morscio J, Dierickx D, Ferreiro JF, et al. Gene expression profiling reveals clear differences between EBV-positive and EBV-negative posttransplant lymphoproliferative disorders. Am. J. Transplant 2013;13(5):1305–1316. [PubMed: 23489474]
29. Morscio J, Tousseyn T. Recent insights in the pathogenesis of post-transplantation lymphoproliferative disorders. World J. Transplant 2016;6(3):505–516. [PubMed: 27683629]
30. Morton CL, Houghton PJ: Establishment of human tumor xenografts in immunodeficient mice. Nat Protoc. 2007;2: 247–250. [PubMed: 17406581]
31. Mosier DE. Immunodeficient mice xenografted with human lymphoid cells: New models for *in vivo* studies of human immunobiology and infectious diseases. J. Clin. Immunol 1990;10(4):185–191. [PubMed: 1976649]
32. Mynarek M, Schober T, Behrends U, Maecker-Kolhoff B. Posttransplant lymphoproliferative disease after pediatric solid organ transplantation. Clin. Dev. Immunol 2013:1–14.
33. Nelson BH. CD20^{+} B Cells: The other tumor-infiltrating lymphocytes. J Immunol. 2010;185(9):4977–4982. [PubMed: 20962266]
34. Pelleitier M, Montplaisir S. The nude mouse: a model of deficient T-cell function. Methods Achiev. Exp. Pathol 1975;7:149–166. [PubMed: 1105061]
35. Quinlan SC, Pfeiffer RM, Morton LM, Engels EA. Risk factors for early-onset and late-onset post-transplant lymphoproliferative disorder in kidney recipients in the United States. Am J Hematol 2011;86: 206–209. [PubMed: 21264909]
36. Radaelli E, Hermans E, Omodho L, et al. Spontaneous post-transplant disorders in NOD.Cg-Prkdc^{scid} Il2rg^{tm1Sug}/JicTac (NOG) mice engrafted with patient-derived metastatic melanomas. PLoS One. 2015;10(5):e0124974–e0124974. [PubMed: 25996609]
37. Ricci F, Bizzaro F, Cesca M, et al. Patient-derived ovarian tumor xenografts recapitulate human clinicopathology and genetic alterations. Cancer Res. 2014;74(23):6980–6990. [PubMed: 25304260]
38. Ruggiu M, Cuccuini W, Mokhtari K, et al. Case report: Central nervous system involvement of human graft versus host disease: Report of 7 cases and a review of literature. Medicine. 2017;96(42):e8303–e8303. [PubMed: 29049232]
39. Schroeder MA, DiPersio JF. Mouse models of graft-versus-host disease: advances and limitations. Dis. Model. & Mech 2011;4(3):318–333.
40. Shulman HM, Kleiner D, Lee SJ, et al. Histopathologic diagnosis of chronic graft-versus-host disease: National Institutes of Health consensus development project on criteria for clinical trials

in chronic graft-versus-host disease: II. Pathology Working Group Report. Biol. Blood Marrow Transplant 2006;12(1):31–47.

41. Shultz LD, Goodwin N, Ishikawa F, Hosur V, Lyons BL, Greiner DL. Human cancer growth and therapy in immunodeficient mouse models. Cold Spring Harb Protoc. 2014;(7):694–708. [PubMed: 24987146]
42. Shultz LD, Lyons BL, Burzenski LM, et al. Human lymphoid and myeloid cell development in NOD/LtSz-scid IL2R^{null} mice engrafted with mobilized human hemopoietic stem cells. J. Immunol 2005;174(10):6477–6489. [PubMed: 15879151]
43. Swerdlow SH, Campo E, Pileri SA, et al. The 2016 revision of the World Health Organization classification of lymphoid neoplasms. Blood. 2016;127(20):2375–2390. [PubMed: 26980727]
44. Tary-Lehmann M, Saxon A, Lehmann PV. The human immune system in hu-PBL-SCID mice. Immunol. Today 1995; 16(11):529–533. [PubMed: 7495490]
45. Tillman H, Janke LJ, Funk A, Vogel P, Rehg JE: Morphologic and Immunohistochemical Characterization of Spontaneous Lymphoma/Leukemia in NSG Mice. Vet Pathol. 2019: 0300985819882631.
46. Triviai I, Ziegler M, Bergholz U, et al. Endogenous retrovirus induces leukemia in a xenograft mouse model for primary myelofibrosis. Proc Natl Acad Sci U S A 111: 8595–8600, 2014. [PubMed: 24912157]
47. van Rijn RS, Simonetti ER, Hagenbeek A, et al. A new xenograft model for graft-versus-host disease by intravenous transfer of human peripheral blood mononuclear cells in RAG2$^{-/-}$–c$^{-/-}$double-mutant mice. Blood. 2003;102(7):2522–2531. [PubMed: 12791667]
48. von Bonin M, Bornhäuser M. Concise Review: The bone marrow niche as a target of graft versus host disease. Stem Cells. 2014;32(6): 1420–1428. [PubMed: 24585665]
49. von Bonin M, Wermke M, Cosgun KN, et al. *In Vivo* expansion of co-transplanted T cells impacts on tumor re-initiating activity of human acute myeloid leukemia in NSG Mice. PLoS One. 2013;8(4):e60680. [PubMed: 23585844]
50. Wachsmuth LP, Patterson MT, Eckhaus MA, Venzon DJ, Gress RE, Kanakry CG. Posttransplantation cyclophosphamide prevents graft-versus-host disease by inducing alloreactive T cell dysfunction and suppression. J Clin. Invest. 2019;129(6):2357–2373. [PubMed: 30913039]
51. Zhang L, Liu Y, Wang X, et al. The extent of inflammatory infiltration in primary cancer tissues is associated with lymphomagenesis in immunodeficient mice. Sci. Rep 2015;5:9447–9447. [PubMed: 25819560]

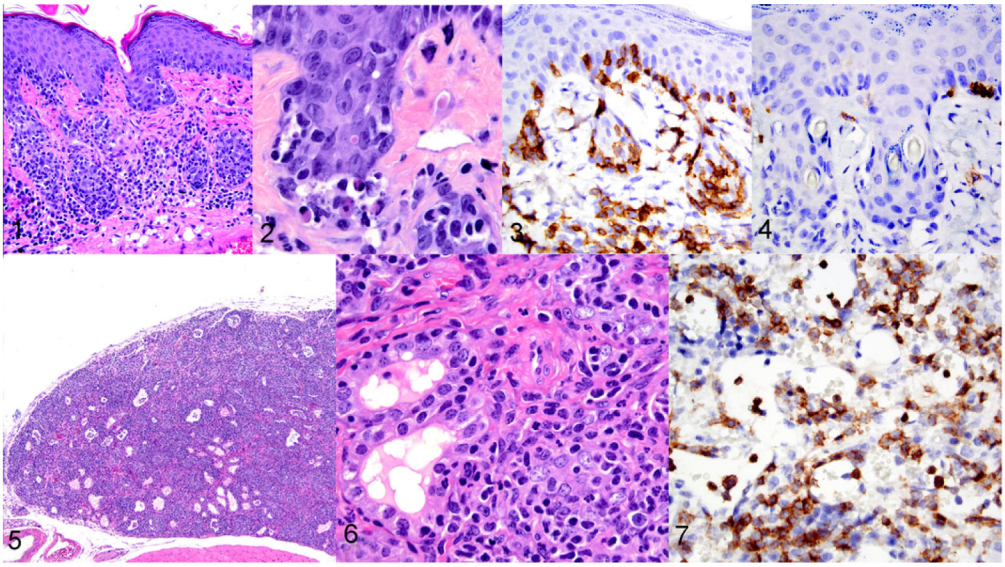

Figures 1–7.

Graft-versus-host disease, mouse, case 5. Figure 1. Skin. Human lymphocytes and plasma cells extend along the dermo-epidermal junction of the epidermis and hair follicles. Haired skin, HE. Figure 2. Higher magnification of Figure 1, showing single cell death and vacuolization of the keratinocytes within the stratum basale. HE. Figures 3 and 4. Skin. GvHD skin lesions are composed of human CD4+ infiltrates (Fig 3) and have fewer human CD8+ infiltrates (Fig 4). IHC. Figure 5 and 6. Thyroid gland. Infiltration, destruction, and effacement of thyroid follicles by lymphocytic infiltrates. HE. Figure 7. Hypoplasia, bone marrow, mouse, case 1. Severe bone marrow hypoplasia due to GvHD. Extensive cellular infiltrates are immunolabeled for human CD4.

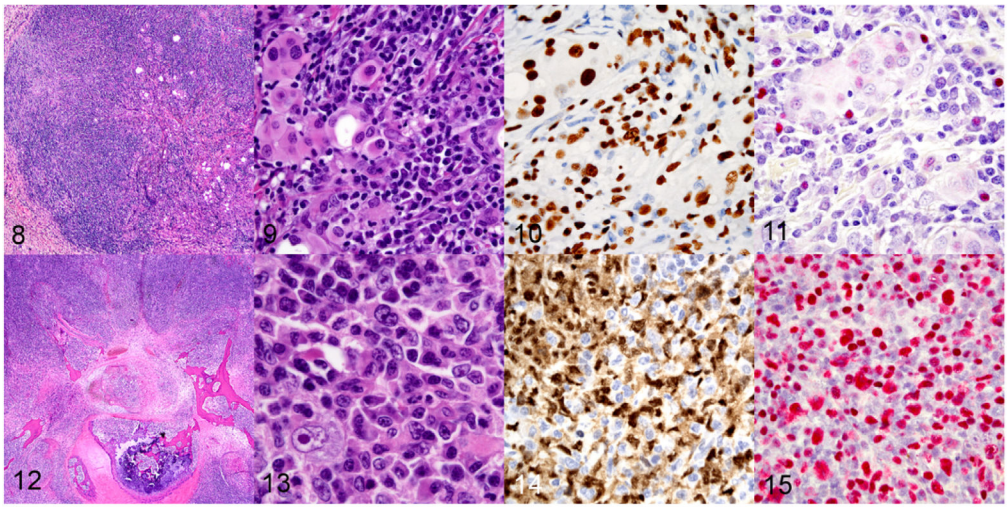

Figures 8–15.

Patient-derived xenograft, subcutaneous site, mouse, case 7. Figure 8. Implanted patient-derived xenograft composed of mixtures of human tumor cells and a human lymphocytic proliferation. Hematoxylin and eosin (HE). Figure 9. Higher magnification of Figure 8, showing multiple human cell subpopulations including engrafted patient-derived solid tumor cells (rhabdomyosarcoma) and lymphoplasmacytic infiltrates. Figure 10. Nuclear immunoreactivity for human-specific NUMA1 in the xenograft tumor (upper left) and lymphoid cells (throughout). Immunohistochemistry. Figure 11. Human lymphocytes express EBERs consistent with EBV infection. *In situ* hybridization. Figures 12-15. EBV-associated monomorphic post-transplant lymphoproliferative disorder in a mouse, case 8. Figure 12. EBV-associated monomorphic post-transplant lymphoproliferation with a large B-cell lymphoma with anaplastic features involving the vertebra and spinal cord. HE. Figure 13. Higher magnification of Figure 12, showing the morphology of the B-cell lymphoma with anaplastic cells. Figure 14. The B-cell lymphoma expresses PAX5. Immunohistochemistry. Fig 15. B-cell lymphoma cells are strongly positive for EBERs. *In situ* hybridization.

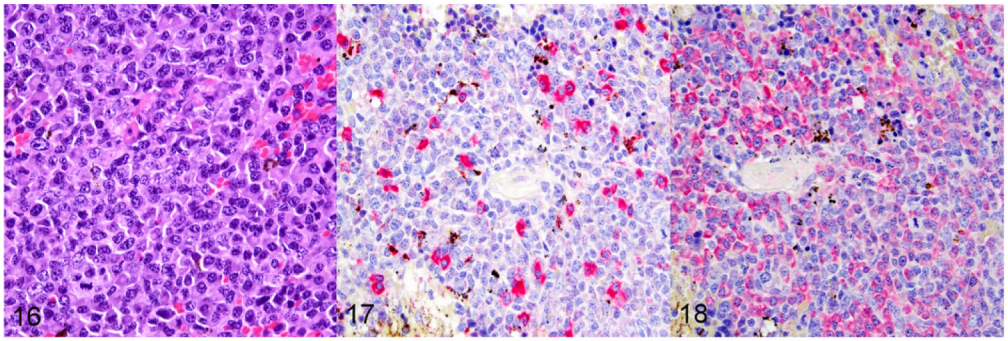

Figure 16–18.
EBV-negative monomorphic post-transplant lymphoproliferative disorder (PTLD) in a mouse spleen, case 4. Figure 16. Monomorphic PTLD characterized by an EBV-negative large B-cell lymphoma. HE. Figure 17. Kappa mRNA is expressed in only a few cells of the B-cell lymphoma. *In situ* hybridization (ISH). Figure 18. Lambda mRNA is expressed in numerous cells of the B-cell lymphoma. ISH.

Table 1.

Primary antibodies, Type, Concentration, Supplier and Technical Procedures for Visualization

Antibody	Type	Concentration	Supplier, Catalog Number
NUMA1 HUMAN	Rabbit polyclonal	1:75	Lifespan Biosciences, LS-B11047[a]
CD3ε	Goat polyclonal	1:1000	Santa Cruz, sc-1127[b]
CD4 HUMAN (4B12)	Mouse monoclonal, IgG1	RTU[c]	Leica, PA0427[d]
CD8 HUMAN (4B11)	Mouse monoclonal, IgG2b	RTU	Leica, PA0183[d]
CD45 HUMAN	Mouse monoclonal, IgG1κ	RTU	Ventana, 760-2505[b]
CD43 HUMAN (DF-T1)	Mouse monoclonal, IgGκ	1:1000	DAKO Agilent, M0786[d]
CD45 MOUSE	Rat LOU/C, LOU/M IgG2bκ	1:500	PharMingen, 553076[b]
CD68 HUMAN (PG-M1)	Mouse monoclonal, IgG3κ	1:50	DAKO Agilent, M0876[e]
CD79a HUMAN (JCB117)	Mouse monoclonal, IgGκ	1:25	DAKO Agilent, M7050[b]
F4/80 (BM8)	Rat, monoclonal, IgG2a	1:500	Invitrogen, MF48000[f]
IRF4	Goat polyclonal	1:4000	Santa Cruz, sc-6059[b]
PAX5	Rabbit monoclonal, IgG	1:1000	Abcam, ab109443[d]

[a] Ventana DISCOVERY ULTRA automated stainer (Ventana Medical Systems, Inc., Tucson, AZ): Heat-induced epitope retrieval (HIER), Cell conditioning media 2 (CC2), 32 minutes at 37°C; Visualization with DISCOVERY OmniMap anti-rabbit HRP (760-4311), DISCOVERY ChromoMap DAB kit (760-159) or DISCOVERY ChromoMap Purple kit (760-229)

[b] Ventana DISCOVERY ULTRA automated stainer (Ventana Medical Systems, Inc.): HIER, Cell conditioning media 1 (CC1), 32 minutes at 37°C; Visualization with biotinylated rabbit anti-mouse IgG secondary antibody (Abcam, ab133469), DISCOVERY OmniMap anti-rabbit HRP (760-4311), DISCOVERY ChromoMap DAB kit (760-159) or DISCOVERY ChromoMap Purple kit (760-229)

[c] RTU: ready to use

[d] Leica BOND-MAX automated stainer (Leica Biosytems, Buffalo Grove, IL): IHC Protocol F. HIER with Bond Epitope Retrieval Solution 2 (ER2) for 20 minutes; Visualization with Bond Polymer Refine Detection (DS9800).

[e] Ventana DISCOVERY ULTRA automated stainer (Ventana Medical Systems, Inc., Tucson, AZ): HIER with CC1, 32 minutes at 37°C; Visualization with IVIEW DAB kit (760-091)

[f] intelliPATH FLX (BioCare Medical, LLC., Pacheco, CA): HIER with Decloaking Chamber NxGen and Target Retrieval, pH 6, 15 minutes at 110 °C (DAKO, S1699, Carpinteria, CA); Visualization with biotinylated rabbit anti-rat IgG, mouse absorbed secondary antibody (Vector Labs, BA-4001); Lab Vision streptavidin peroxidase (Thermo Scientific, TS-125-HR); DAB chromogen kit (Thermo Scientific, TA-125-QHDX)

Table 2.

In situ Probes Supplier and Technical Procedures for Visualization

Probe	Type	Supplier, Catalog Number
EBER[a]	Epstein-Barr Virus encoded RNA (EBER)	Leica Biosystems, PB0589
Kappa light chain[a]	Kappa light chain mRNA, Human specific	Leica Biosystems, PB0645
Lambda light chain[a]	Lambda light chain mRNA, Human specific	Leica Biosystems, PB0669

[a]Leica BOND-MAX automated stainer (Leica Biosystems, Buffalo Grove, IL). ISH Protocol A. Bond Enzyme Pretreatment Kit (AR9551), Enzyme 1, for 15 minutes. Bond Polymer Refine Red Detection Kit (DS9390).

Table 3.

Clinical Data for NSG Mice Engrafted with Human Pediatric Solid Tumors

Case	Gender	Age (weeks)	Microbiology testing	Leukocyte count	PDX	Days on study	EBER ISH	Xenograft
1	Female	15	Blood culture[a,b]	4.18 X 10^3/μL	Hepatoblastoma	47	−	+[c]
2	Female	14	n/d	n/d	Osteosarcoma	54	−	−
3	Female	14	Blood culture[d]	7.72 X 10^3/μL	Rhabdomyosarcoma	34	−	−
4	Female	32	Blood culture[d]; Lung culture[a]	86.74 X 10^3/μL	Hepatoblastoma	61	−	−
5	Female	16	Blood culture[e,f]	2.98 X 10^3/μL	Malignant Thymoma	46	+	+[c]
6	Female	17	Blood culture[f,g]; Lung culture[g]	0.82 X 10^3/μL	Rhabdomyosarcoma[h]	60	+	−
7	Female	17	Lung culture[d]; Synovial culture[b,f]	8.3 X 10^3/μL	Rhabdomyosarcoma[h]	60	+	+
8	Female	28	Blood culture[b,i]	4.06 X 10^3/μL	Hepatoblastoma	124	+	+
9	Female	21	Blood culture[d]	3.92 X 10^3/μL	Osteosarcoma[h]	64	−	−
10	Female	52	Blood culture[a]	1.24 X 10^3/μL	Osteosarcoma	283	−	−
11	Female	26	Blood culture[d]	4.08 X 10^3/μL	Osteosarcoma[h]	99	−	−

a: Klebsiella pneumoniae

b: Staphylococcus lentus

c: resolving tumor

d: no growth

e: Rothia mucilaginosa

f: Streptococcus parasanguinis

g: Actinomyces meyeri

h: Portions of the same patient tumor type (as listed) were implanted into separate mice

i: Staphylococcus xylosus

PDX: patient derived xenograft, EBER: EBV-encoded small RNAs, ISH: *in situ* hybridization

Table 4.

Anatomic Distribution of Lymphoproliferations in NSG Mice following PDX Transplantation

Case	Lung	Eso[a]	Ton	Thg	Salv	Stom	SI	LI	CNS	BM	Liver	Kid	Spl	LNC	Skin	MC
1	+	+	+	+	+	+	–	–	+	+	+	+	–	+[b]	+	+
2	+	+	–	+	+	+	–	–	–	+	+	+	+	+[b]	+	+
3	+	–	–	–	–	–	–	–	–	–	+	–	+	+	–	–
4[c]	+[d]	+[d]	+[d]	+[d]	+[d]	+[d]	–	–	–	–	+[d]	+[d]	+[d]	+[d]	+[d]	+[d]
5[e]	+[d]	+[d]	+[d]	+[d]	+[d]	+[d]	–	–	+	–	+[d,f]	+	+[d,f]	+	+[d]	+[d]
6[e]	+[d]	+[d]	+[d]	+[d]	+[d]	+[d]	–	–	+	–	+[d,f]	–	+[d,f]	–	+[d]	+[d]
7[e]	+[d]	+[d]	+[d]	+[d]	+[d]	+[d]	–	–	+	+[d]	+[d,f]	–	+/min[f]	n/t	+[d]	+[d]
8[c]	–	–	–	–	–	–	–	–	+[d]	–	+[d,f]	–	+[d,f]	–	–	–
9	+	+	+	+	+	+	+	–	+	–	+	+	+	+[b]	+	+
10	+/min	–	–	–	–	–	–	–	–	–	+/min	–	–	n/t	+	–
11	+	–	–	+	+	–	+	–	+	–	+	+	+	+[b]	+	+
Total	**11**	**8**	**6**	**8**	**8**	**7**	**2**	**0**	**7**	**3**	**11**	**6**	**9**	**7**	**9**	**8**

Abbreviation n/t: no tissue available

a: Eso: Esophagus, Ton: tongue, Thg: thyroid gland, Salv: salivary gland, Stom: stomach, SI: small intestines, LI: large intestines, CNS: central nervous system, BM: bone marrow, Kid: kidney, Spl spleen, LNC: cervical lymph node, MC: mucocutaneous junctions; min: minimal infiltration of tissue by immune cells

b: sclerosis observed

c: monomorphic PTLD

d: PTLD present

e: polymorphic PTLD

f: EBV-positive by ISH

PTLD: post-transplantation lymphoproliferative disorder, PDX: patient derived xenograft, EBER: EBV-encoded small RNAs, ISH: *in situ* hybridization